

REPORT DOCUMENTATION PAGE			Form Approved OMB NO. 0704-0188		
<p>The public reporting burden for this collection of information is estimated to average 1 hour per response, including the time for reviewing instructions, searching existing data sources, gathering and maintaining the data needed, and completing and reviewing the collection of information. Send comments regarding this burden estimate or any other aspect of this collection of information, including suggestions for reducing this burden, to Washington Headquarters Services, Directorate for Information Operations and Reports, 1215 Jefferson Davis Highway, Suite 1204, Arlington VA, 22202-4302. Respondents should be aware that notwithstanding any other provision of law, no person shall be subject to any penalty for failing to comply with a collection of information if it does not display a currently valid OMB control number. PLEASE DO NOT RETURN YOUR FORM TO THE ABOVE ADDRESS.</p>					
1. REPORT DATE (DD-MM-YYYY) 22-12-2015		2. REPORT TYPE Final Report		3. DATES COVERED (From - To) 1-Jan-2015 - 30-Sep-2015	
4. TITLE AND SUBTITLE Final Report: STIR Proposal For Research Area 2.1.2 Surface Energy Balance: Transient Soil Density Impacts Land Surface Characteristics And Characterization			5a. CONTRACT NUMBER W911NF-14-1-0655		
			5b. GRANT NUMBER		
			5c. PROGRAM ELEMENT NUMBER 611102		
6. AUTHORS Joshua L. Heitman			5d. PROJECT NUMBER		
			5e. TASK NUMBER		
			5f. WORK UNIT NUMBER		
7. PERFORMING ORGANIZATION NAMES AND ADDRESSES North Carolina State University 2701 Sullivan Drive Admin Services III; Box 7514 Raleigh, NC 27695 -7514			8. PERFORMING ORGANIZATION REPORT NUMBER		
9. SPONSORING/MONITORING AGENCY NAME(S) AND ADDRESS (ES) U.S. Army Research Office P.O. Box 12211 Research Triangle Park, NC 27709-2211			10. SPONSOR/MONITOR'S ACRONYM(S) ARO		
			11. SPONSOR/MONITOR'S REPORT NUMBER(S) 66053-EV-II.2		
12. DISTRIBUTION AVAILABILITY STATEMENT Approved for Public Release; Distribution Unlimited					
13. SUPPLEMENTARY NOTES The views, opinions and/or findings contained in this report are those of the author(s) and should not be construed as an official Department of the Army position, policy or decision, unless so designated by other documentation.					
14. ABSTRACT Soil density is commonly treated as static in studies on land surface property dynamics. Magnitudes of errors associated with this assumption are largely unknown. Objectives of this preliminary investigation were to: i) quantify effects of soil density variation on soil properties, and ii) evaluate impact of changing soil density on surface energy balance and heat and water transfer. Six soil properties were evaluated over a range of soil densities, using a combination of ten modeling approaches. Thermal conductivity, water characteristics, hydraulic conductivity, and vapor diffusivity were most sensitive; these properties changed by fractions greater than					
15. SUBJECT TERMS Soil, hydrology, surface energy balance					
16. SECURITY CLASSIFICATION OF:		17. LIMITATION OF ABSTRACT	15. NUMBER OF PAGES	19a. NAME OF RESPONSIBLE PERSON	
a. REPORT	b. ABSTRACT			c. THIS PAGE	Joshua Heitman
UU	UU	UU		19b. TELEPHONE NUMBER 919-513-1593	



## Report Title

Final Report: STIR Proposal For Research Area 2.1.2 Surface Energy Balance: Transient Soil Density Impacts Land Surface Characteristics And Characterization

### ABSTRACT

Soil density is commonly treated as static in studies on land surface property dynamics. Magnitudes of errors associated with this assumption are largely unknown. Objectives of this preliminary investigation were to: i) quantify effects of soil density variation on soil properties, and ii) evaluate impact of changing soil density on surface energy balance and heat and water transfer. Six soil properties were evaluated over a range of soil densities, using a combination of ten modeling approaches. Thermal conductivity, water characteristics, hydraulic conductivity, and vapor diffusivity were most sensitive; these properties changed by fractions greater than associated change in density (i.e., 10% change in density led to >10% change in property). Subsequently, three field seasons were simulated with a numerical model (HYDRUS-1D) for a range of bulk densities. Among the surface energy balance terms, ground heat flux and latent heat flux were most sensitive to bulk density. Surface soil temperature variation increased in with low bulk densities but subsurface temperature variation decreased. Surface water content varied with bulk density but effects mostly disappeared in the subsurface. Results demonstrate significance of transient density on surface conditions and point to need for continued evaluation of impacts with improved measurements and modeling.

---

**Enter List of papers submitted or published that acknowledge ARO support from the start of the project to the date of this printing. List the papers, including journal references, in the following categories:**

**(a) Papers published in peer-reviewed journals (N/A for none)**

<u>Received</u>	<u>Paper</u>
-----------------	--------------

**TOTAL:**

**Number of Papers published in peer-reviewed journals:**

---

**(b) Papers published in non-peer-reviewed journals (N/A for none)**

<u>Received</u>	<u>Paper</u>
-----------------	--------------

**TOTAL:**

**Number of Papers published in non peer-reviewed journals:**

---

### (c) Presentations

Kojima, Y., J.L. Heitman, and R. Horton. 2015. Numerical Evaluation of Transient Density Impact on Surface Energy Balance and Coupled Heat and Water Transfer in Soils. Grand Challenges in Modeling Soil Processes. Soil Science Society of America International Meeting, Minneapolis, MN. November 16, 1015.

Number of Presentations: 1.00

---

**Non Peer-Reviewed Conference Proceeding publications (other than abstracts):**

Received      Paper

**TOTAL:**

Number of Non Peer-Reviewed Conference Proceeding publications (other than abstracts):

---

**Peer-Reviewed Conference Proceeding publications (other than abstracts):**

Received      Paper

**TOTAL:**

Number of Peer-Reviewed Conference Proceeding publications (other than abstracts):

---

**(d) Manuscripts**

Received      Paper

12/22/2015    1.00    Lalit Arya, Joshua Heitman. A Non-Empirical Method for Computing Pore Radii and Soil Water Characteristics from Particle-Size Distribution, Soil Science Society of America Journal (04 2015)

**TOTAL:      1**

Number of Manuscripts:

---

**Books**

Received      Book

**TOTAL:**

Received      Book Chapter

**TOTAL:**

**Patents Submitted**

---

**Patents Awarded**

---

**Awards**

---

**Graduate Students**

<u>NAME</u>	<u>PERCENT SUPPORTED</u>
<b>FTE Equivalent:</b>	
<b>Total Number:</b>	

**Names of Post Doctorates**

<u>NAME</u>	<u>PERCENT SUPPORTED</u>
Xinhua Xiao	0.75
Yuki Kojima	0.00
<b>FTE Equivalent:</b>	<b>0.75</b>
<b>Total Number:</b>	<b>2</b>

**Names of Faculty Supported**

<u>NAME</u>	<u>PERCENT SUPPORTED</u>	National Academy Member
Joshua L. Heitman	0.04	
<b>FTE Equivalent:</b>	<b>0.04</b>	
<b>Total Number:</b>	<b>1</b>	

**Names of Under Graduate students supported**

<u>NAME</u>	<u>PERCENT SUPPORTED</u>
<b>FTE Equivalent:</b>	
<b>Total Number:</b>	

**Student Metrics**

This section only applies to graduating undergraduates supported by this agreement in this reporting period

The number of undergraduates funded by this agreement who graduated during this period: ..... 0.00

The number of undergraduates funded by this agreement who graduated during this period with a degree in science, mathematics, engineering, or technology fields:..... 0.00

The number of undergraduates funded by your agreement who graduated during this period and will continue to pursue a graduate or Ph.D. degree in science, mathematics, engineering, or technology fields:..... 0.00

Number of graduating undergraduates who achieved a 3.5 GPA to 4.0 (4.0 max scale):..... 0.00

Number of graduating undergraduates funded by a DoD funded Center of Excellence grant for Education, Research and Engineering:..... 0.00

The number of undergraduates funded by your agreement who graduated during this period and intend to work for the Department of Defense ..... 0.00

The number of undergraduates funded by your agreement who graduated during this period and will receive scholarships or fellowships for further studies in science, mathematics, engineering or technology fields:..... 0.00

**Names of Personnel receiving masters degrees**

<u>NAME</u>
<b>Total Number:</b>

**Names of personnel receiving PHDs**

<u>NAME</u>
<b>Total Number:</b>

**Names of other research staff**

<u>NAME</u>	<u>PERCENT SUPPORTED</u>
<b>FTE Equivalent:</b>	
<b>Total Number:</b>	

**Sub Contractors (DD882)**

**Inventions (DD882)**

**Scientific Progress**

**Technology Transfer**

See Attachment

***STIR PROJECT:***  
**TRANSIENT SOIL DENSITY IMPACTS LAND SURFACE CHARACTERISTICS AND  
CHARACTERIZATION**

**Y. Kojima, J.L. Heitman (PI), and R. Horton**

**ABSTRACT**

Soil density is commonly treated as static in studies on land surface property dynamics. Magnitudes of errors associated with this assumption are largely unknown. Objectives of this preliminary investigation were to: i) quantify effects of soil density variation on soil properties, and ii) evaluate impact of changing soil density on surface energy balance and heat and water transfer. Six soil properties were evaluated over a range of soil densities, using a combination of ten modeling approaches. Thermal conductivity, water characteristics, hydraulic conductivity, and vapor diffusivity were most sensitive; these properties changed by fractions greater than associated change in density (i.e., 10% change in density led to >10% change in property). Subsequently, three field seasons were simulated with a numerical model (HYDRUS-1D) for a range of bulk densities. Among the surface energy balance terms, ground heat flux and latent heat flux were most sensitive to bulk density. Surface soil temperature variation increased in with low bulk densities but subsurface temperature variation decreased. Surface water content varied with bulk density but effects mostly disappeared in the subsurface. Results demonstrate significance of transient density on surface conditions and point to need for continued evaluation of impacts with improved measurements and modeling.

## INTRODUCTION

Surface soil is a complex, dynamic interface which dictates mass and energy transfer between land and atmosphere, and determines water flow and partitioning in the hydrological cycle. Its properties are considered dynamic because they are controlled in part by soil water content, which can change quickly with wetting events or slowly over sustained periods of drainage, plant uptake, and evaporative drying. Filling and emptying of water in soil pore space alters soil hydraulic and thermal properties. Because understanding soil-water controlled properties is critical for modeling and interpreting broader hydrologic and environmental processes, tremendous effort has been expended to develop soil water sensor technologies and monitoring networks (Robinson et al., 2008; Ochsner et al., 2013). This work has led to new understanding of soil property dynamics, and for potentially even greater understanding, as these measurements are coupled with remote sensing to extend measurement footprints (Albergel et al., 2012). Yet, in all of these efforts there remain fundamental questions that have not been addressed. An elementary and ubiquitous assumption in hydrologic studies considering dynamic soil surface properties is that soil density is static. We know, in fact, that this is not the case.

Consequences associated with this assumption are largely unknown, but are likely critical (cf. Arya and Paris, 1981; Moldrup et al., 2000; Ochsner et al., 2001). Large areas of the land surface undergo significant changes in surface soil density through annual cycles of disturbance associated with agriculture (Strudley et al., 2008; Logsdon, 2012; Liu et al., 2014). Freeze-thaw processes alter surface density and arrangement seasonally (Staricka and Benoit, 1995). Shrink-swell processes, erosion, and deposition alter surface soil density and arrangement episodically (Timm et al., 2006). Unfortunately, due to historical, practical limitations in our ability to continuously quantify soil density-derived effects, this limitation remains mostly unaddressed as a dynamic factor in land surface characterization, and the magnitudes of any associated errors are unknown to scientists and engineers working on a multitude of related investigations.

Our general goal is to examine the impact of transient (i.e., dynamic) soil density on land surface characteristics and characterization. Moving forward toward this goal likely requires both extensive measurement and modeling efforts. The objectives for this STIR project were focused toward making initial progress in work aimed at this longer-term goal.

Specific objectives for this project were to:

- 1) Quantify effects of soil density variation on fundamental soil properties.
- 2) Evaluate impact of changing soil density and associated properties on surface energy balance and coupled heat and water transfer in soils.

We first modeled a series of germane soil properties: volumetric heat capacity, thermal conductivity, soil thermal diffusivity, water retention characteristics, hydraulic conductivity, and vapor diffusivity using soil property models from the literature that included the capacity to incorporate bulk density dependence. We then used a subset of these properties in a numerical model to examine expected variation in surface energy balance terms, soil water content, and soil temperature associated with bulk density variation as a case study. In the following, methods and results are summarized together by analysis. Detailed interpretation is currently being pursued for a forthcoming manuscript.

## PROPERTY MODELING (Objective 1)

We based our analysis on the range of bulk densities ( $\rho_b$ ) observed in several previous field studies. Berndt and Coughlam (1976) investigated  $\rho_b$  changes associated with shrink-swell of a clay soil and reported values ranging from 1.04 to 1.37 Mg m<sup>-3</sup> (32% variation) with wetting-drying cycles. Kays et al. (1985) showed, for a clay loam soil, that  $\rho_b$  change associated with freeze-thaw cycles was from 1.28 to 1.18 Mg m<sup>-3</sup> (8% variation). Logsdon (2012) observed  $\rho_b$  variation, through periodic sampling over 5 yr in a clay loam, of 1.25 to 1.40 Mg m<sup>-3</sup> (12% variation). Liu et al. (2014) observed  $\rho_b$  variations due to settling after tillage and reported values for silt loam changing from 1.00 to 1.35 Mg m<sup>-3</sup> (35% change), and values for a sandy loam changed from 1.10 to 1.35 Mg m<sup>-3</sup> (23% change).

We tested three soils in our analysis (Table 1): silt loam and sandy loam with data from Liu et al. (2014), and clay loam from Logsdon et al. (2012) using properties of a Webster soil series.

### Soil Thermal Properties

Impact of  $\rho_b$  on soil *volumetric heat capacity*  $C$  was evaluated with the de Vries (1963) model,

$$C = c_s \rho_b + C_L \theta \quad [1]$$

where  $c_s$  is specific heat of soil solid (J kg<sup>-1</sup> °C<sup>-1</sup>),  $C_L$  is volumetric heat capacity of liquid water (4,184,000 J m<sup>-3</sup> K<sup>-1</sup>) and  $\theta$  is volumetric water content (m<sup>3</sup> m<sup>-3</sup>). The values for  $c_s$  were calculated based on particle size distribution and soil organic matter content (SOM) as described by de Vries (1963). The  $C$  values were calculated for  $\theta = 0.10$  m<sup>3</sup> m<sup>-3</sup> to 0.40 m<sup>3</sup> m<sup>-3</sup> and with  $\rho_b = 1.10$  Mg m<sup>-3</sup> to 1.40 Mg m<sup>-3</sup>.

As would be expected from the model, increasing  $\rho_b$  resulted in an increase of  $C$ , and the rate of increase was constant over the range of  $\theta$  (Fig. 1). If we treat our minimum  $\rho_b$  as the standard and use  $\theta = 0.25$  m<sup>3</sup> m<sup>-3</sup> for evaluation, a 100 kg m<sup>-3</sup> increase in  $\rho_b$  results in 77-84 kJ m<sup>-3</sup> K<sup>-1</sup> increase in  $C$ . In percent, approximately 8% increase in  $\rho_b$  resulted in 4.0, 4.1, and 4.0 % increase in  $C$  for clay loam, silt loam, and sandy loam, respectively. The  $C$  values for observed maximum  $\rho_b$  were 106%, 110%, and 108% of the values for observed minimum  $\rho_b$  for clay loam, silt loam, and sandy loam, respectively.

Impact of  $\rho_b$  on soil *thermal conductivity*  $\lambda$  was evaluated with the de Vries (1963), Campbell (1985), and Lu et al. (2014) models. de Vries (1963) provided an equation to calculate  $\lambda$  based on the soil particle size distribution,  $\rho_b$ , and soil organic matter content:

$$\lambda = \frac{\sum_{i=0}^N k_i x_i \lambda_i}{\sum_{i=0}^N k_i x_i} \quad [2]$$

where  $N$  is the number of types of soil constituents,  $k_i$  is a weighting factor,  $x_i$  is volume fraction, and  $\lambda_i$  is thermal conductivity of each soil constituent. Empirically determined values for  $k_i$  were used in this study.

Campbell (1985) provided the following equation

$$\lambda = A + B\theta - (A - D) \exp[-(E\theta)^4] \quad [3]$$

where  $A$ ,  $B$ ,  $D$ , and  $E$  are shape factors associated with soil properties. Empirical parameters can be calculated as:

$$A = \frac{0.57 + 1.73\theta_q + 0.93\theta_m}{1 - 0.74\theta_q - 0.49\theta_m} - 2.8\theta_{\text{solid}}(1 - \theta_{\text{solid}}) \quad [4]$$

$$B = 2.8\theta_{\text{solid}} \quad [5]$$

$$D = 0.03 + 0.7\theta_{\text{solid}} \quad [6]$$

$$E = 1 + 2.6m_c^{-0.5} \quad [7]$$

where  $\theta_q$  is volume fraction of quartz,  $\theta_m$  is volume fraction of other minerals,  $\theta_{\text{solid}}$  is volume fraction of soil solid, and  $m_c$  is clay fraction. This model does not account for soil organic matter. In this study we assumed that  $\theta_q$  is equal to volume fraction of sand, and  $\theta_m$  is equal to the volume fraction of silt plus clay.

Lu et al. (2014) provided the following equation

$$\lambda = \lambda_{\text{dry}} + \exp(\beta - \theta^{-\alpha}) \quad [8]$$

where  $\lambda_{\text{dry}}$  is thermal conductivity of oven dried soil, and  $\alpha$  and  $\beta$  are shape factors. The thermal conductivity of oven dried soil can be estimated from soil porosity  $\tau$ .

$$\lambda_{\text{dry}} = -0.56\tau + 0.51 \quad [9]$$

The shape factors  $\alpha$  and  $\beta$  can be determined based on soil particle distribution and  $\rho_b$

$$\alpha = 0.67f_{\text{cl}} + 0.24 \quad [10]$$

$$\beta = 1.97f_{\text{sa}} + 0.00187\rho_b - 0.00136f_{\text{sa}}\rho_b - 0.95 \quad [11]$$

where  $f_{\text{cl}}$  is clay mass fraction,  $f_{\text{sa}}$  is sand mass fraction.

For the de Vries (1963) model,  $\lambda$  increases with increases of  $\rho_b$  and  $\theta$  (Fig. 2). Values of  $\lambda$  were highest for sandy loam, and lowest for silt loam (sandy loam > clay loam > silt loam). When  $\theta = 0.25 \text{ m}^3 \text{ m}^{-3}$ , a  $100 \text{ kg m}^{-3}$  (8%) increase in  $\rho_b$  results in 12.8%, 11.9%, and 14.4% increases in  $\lambda$  for clay loam, silt loam, and sandy loam, respectively. The  $\lambda$  values for observed maximum  $\rho_b$  were 122%, 140%, and 131% of the values for observed minimum  $\rho_b$  for clay loam, silt loam, and sandy loam, respectively.

The Campbell (1985) model is shown in Fig. 3. Trends were similar to those from the de Vries (1963) model, but values of  $\lambda$  were generally larger. Values of  $\lambda$  were highest for sandy loam, and lowest for silt loam (sandy loam > silt loam > clay loam). With  $\theta = 0.25 \text{ m}^3 \text{ m}^{-3}$ , a  $100 \text{ kg m}^{-3}$  increase in  $\rho_b$  caused 11.2%, 11.0%, and 11.8% increases of  $\lambda$  for clay loam, silt loam, and sandy loam, respectively. The  $\lambda$  values for observed maximum  $\rho_b$  were 117%, 130%, and 125% of the values for observed minimum  $\rho_b$  for clay loam, silt loam, and sandy loam, respectively. These percentage increases are smaller than those with the de Vries model, despite similar changes in  $\lambda$ , because of generally higher  $\lambda$  values for the Campbell model.

The Lu et al. (2014) model followed similar trends as the other models (Fig. 4). With  $\theta = 0.25 \text{ m}^3 \text{ m}^{-3}$ , a  $100 \text{ kg m}^{-3}$  increase in  $\rho_b$  caused 15.4%, 16.4%, and 12.0% increases in  $\lambda$  for clay loam, silt loam, and sandy loam, respectively. The  $\lambda$  values for observed maximum  $\rho_b$  were 124%, 146%, and 125% of the values for observed minimum  $\rho_b$  for clay loam, silt loam, and sandy loam, respectively.

**Thermal diffusivity**  $\kappa$  ( $=\lambda/C$ ) was calculated as a function of  $\rho_b$  and  $\theta$  based on the de Vries (1963) model for  $C$  and Campbell (1985) model for  $\lambda$  (Fig. 5). The effect of  $\rho_b$  is very small with  $\theta < 0.15 \text{ m}^3 \text{ m}^{-3}$  for clay loam and silt loam, but generally increases in  $\rho_b$  resulted in increases in  $\kappa$ . With  $\theta = 0.25 \text{ m}^3 \text{ m}^{-3}$ , a  $100 \text{ kg m}^{-3}$  increase in  $\rho_b$  caused 7.0%, 6.6%, and 7.5% increases in  $\kappa$  for clay loam, silt loam, and sandy loam, respectively. The  $\kappa$  values for observed maximum  $\rho_b$  were 111%, 118%, and 116% of values for observed minimum  $\rho_b$  for clay loam, silt loam, and sandy loam, respectively.

### Soil Hydraulic Properties

**Water characteristics** were first examined at different values of  $\rho_b$  and  $\theta$  using ROSETTA, which is a hierarchical pedotransfer function (Schaap et al., 2001). Empirical parameters for the van Genuchten (1980) water retention model:  $\theta_s$ ,  $\theta_r$ ,  $\alpha$ , and  $n$  are output by ROSETTA. ROSETTA also outputs saturated hydraulic conductivity  $K_s$ . The van Genuchten (1980) model is

$$\theta = \theta_r + (\theta_s - \theta_r) \left[ \frac{1}{1 + |\alpha\psi|^n} \right]^{1-1/n} \quad [12]$$

where  $\psi$  (m) is soil water matric potential,  $\theta_s$  and  $\theta_r$  are often referred to as saturated and residual water contents, respectively.

Increases in  $\rho_b$  caused decreases in  $\theta_r$ ,  $\theta_s$ , and  $K_s$  (Table 2). Decreases in  $\theta_s$  and  $K_s$  are reasonable but values for  $\theta_r$  are expected to increase because of reduction of pore size (Assouline, 2006a). Figure 6 shows resulting soil water retention curves as a function of  $\rho_b$  and  $\psi$ . Increases in  $\rho_b$  shift the water retention curves downward. A significant impact of  $\rho_b$  increase is shown clearly in the decrease of saturated water contents. There are also relatively large differences in matric potential when soil is dry. With  $\psi = -10 \text{ m}$ , water content decreased  $0.002\text{-}0.008 \text{ m}^3 \text{ m}^{-3}$  for a  $100 \text{ kg m}^{-3}$  increase in  $\rho_b$ . Impact of altering  $\rho_b$  is more significant in finer textured soil, i.e., clay loam.

The effect of  $\rho_b$  changes on water characteristics was also tested with the model suggested by Assouline (2006a). Assouline (2006a) described the water retention curve as

$$S_e = 1 - \exp \left\{ - \left[ \alpha \left( |\psi|^{-1} - |\psi_L|^{-1} \right) \right]^\mu \right\} \quad [13]$$

where  $S_e$  is degree of saturation,  $S_e = (\theta - \theta_r) / (\theta_s - \theta_r)$ ,  $\alpha$  and  $\mu$  are fitting parameters,  $\psi_L$  is matric potential corresponding to a very small water content,  $\theta_L$ , which represents the limit of the domain of interest of the water retention curve. For convenience,  $\theta_r$  can be assumed to equal  $\theta_L$ .

Brooks and Corey (1964) suggested the following expression of the water retention curve

$$\begin{aligned} S_e &= (\psi/\psi_a)^{-\sigma} & \psi < \psi_a \\ S_e &= 1 & \psi \geq \psi_a \end{aligned} \quad [14]$$

where  $\psi_a$  is air entry pressure, and  $\sigma$  is a pore-size distribution index. Assouline showed that  $\sigma$  is related to parameters in Eq. [13]

$$\sigma = 0.81\epsilon^{-0.837} \quad [15]$$

$$\varepsilon = \frac{(\alpha^\mu)^{-1/\mu} \Gamma(1 + 1/\mu) + 1/|\psi_L|}{\{(\alpha^\mu)^{-2/\mu} [\Gamma(1 + 2/\mu) - \Gamma^2(1 + 1/\mu)]\}^{1/2}} \quad [16]$$

Assouline (2006a) presented equations where water retention curves at varying  $\rho_b$  can be estimated when fitting parameters  $\alpha$ ,  $\mu$ , and  $\psi_a$  are determined with experimental data at one  $\rho_b$ . The parameters in Eqs. [13]-[14] for the new water retention curve with different  $\rho_b$ ,  $\alpha_c$ ,  $\mu_c$ , and  $\psi_{ac}$ , are described as

$$\alpha_c = \alpha(\rho_{bc} / \rho_b)^{3.72} \quad [17]$$

$$\mu_c = \mu(\rho_{bc} / \rho_b)^\omega \quad [18]$$

$$\psi_{ac} = \psi_a(\rho_{bc} / \rho_b)^{3.82} \quad [19]$$

where  $\rho_b$  and  $\rho_{bc}$  are original and new bulk densities, and  $\omega$  is defined as

$$\omega = 2.3 - 1.9(SC / CC)^{-0.5} \quad [20]$$

where SC and CC are mass fraction of silt and clay. The values for  $\theta_s$  and  $\theta_r$  also change with changes in  $\rho_b$ . Assouline (2006a) presented

$$\theta_{sc} = \theta_s [(\rho_s - \rho_{bc}) / (\rho_s - \rho_b)] \quad [21]$$

$$\theta_{rc} = \theta_r (\rho_{bc} / \rho_b) \quad [22]$$

where  $\theta_{sc}$  and  $\theta_{rc}$  are saturated and residual water content with the new  $\rho_b$  value, and  $\rho_s$  is soil solid density ( $\approx 2650 \text{ kg m}^{-3}$ ).

In this study, we first obtained water retention parameters for the van Genuchten (1980) model from ROSETTA for clay loam, silt loam, and sandy loam at  $\rho_b = 1.25 \text{ Mg m}^{-3}$ . Parameters for Eqs. [13]-[14] were determined by fitting data from these water retention curves. Based on these parameters and new  $\rho_b$ , water retention curves were estimated with Eqs. [15]-[21].

Table 3 shows a subset of the parameters required for Eqs. [12]-[14] at different  $\rho_b$ . Estimates of  $\theta_r$  were plausible by this approach in that  $\theta_r$  decreases as  $\rho_b$  decreases. Thus, the water retention curves with different  $\rho_b$  values cross one another (Fig. 7). At the same  $\psi$ , water content sometimes increased and sometimes decreased, depending on  $\psi$  and soil type. For example, when  $\psi = -1 \text{ m}$  and with a  $100 \text{ kg m}^{-3}$  increase in  $\rho_b$ , water content increased 0.02 in clay loam, water content decreased 0.03 in silt loam, and water content increased 0.01-0.02 in sandy loam. When  $\psi = -10 \text{ m}$  and with a  $100 \text{ kg m}^{-3}$  increase in  $\rho_b$ , water content increased 0.004 in clay loam, water content decreased 0.004 in silt loam, and water content decreased 0.01 in sandy loam.

**Hydraulic conductivity**  $K$  can be expressed by the van Genuchten model (1980) and parameters provided by ROSETTA as

$$K(S_e) = K_s S_e^{0.5} \left[ 1 - (1 - S_e^{1/m})^m \right]^p \quad [23]$$

where  $S_e$  for Eq. [23] is

$$S_e = \left[ \frac{1}{1 + |\alpha\psi|^n} \right]^{1-1/n} \quad [24]$$

Hydraulic conductivity as a function of  $\psi$  and  $\rho_b$  is shown in Fig 8 (and  $K_s$  is given in Table 2). As would be expected,  $K$  consistently decreased with increasing  $\rho_b$ .

Assouline (2006b) presented an alternate model to describe  $K_s$  as a function of  $\rho_b$ , the value  $K_{sc}$  is

$$K_{sc} = K_s \left( \frac{\theta_{sc} - \theta_{rc}}{\theta_s - \theta_r} \right)^{2.5} \left( \frac{\psi_a}{\psi_{ac}} \right)^2 \left[ \frac{\sigma_c(1 + \sigma)}{\sigma(1 + \sigma_c)} \right]^2 \quad [25]$$

where  $K_s$ ,  $\theta_s$ ,  $\theta_r$ ,  $\psi_a$ , and  $\sigma$  are saturated hydraulic conductivity, saturated water content, residual water content, air entry pressure, and pore size distribution index at standard  $\rho_b$ , and  $\theta_{sc}$ ,  $\theta_{rc}$ ,  $\psi_{ac}$ , and  $\sigma_c$  are saturated water content, residual water content, air entry pressure, and pore size distribution index at the new  $\rho_b$ . Unsaturated hydraulic conductivity  $K(S_e)$  for a variety of  $\rho_b$  were estimated with the Mualem (1976) and Brooks and Corey (1964) model

$$K(S_e) = K_s S_e^{(2+2.5\sigma)/\sigma} \quad [26]$$

Values of  $K_s$  for different  $\rho_b$  are shown in Table 3. Note that  $K_s$  at  $1.25 \text{ Mg m}^{-3}$  was used as the standard for modification at other  $\rho_b$  according to Eq. [26]. Figure 9 shows  $K$  estimated with Eqs. [25] and [26] as a function of  $\rho_b$  and  $\psi$  instead of  $S_e$ . Relative effects --  $K$  decreases with increasing  $\rho_b$  -- are similar to those obtained from ROSETTA, despite differences in the water characteristics discussed earlier because the Mualem model treats residual water content as immobile.

**Vapor diffusivity**  $D_v$  in soil can be described as (Saito et al., 2006)

$$D_v = \tau \theta_a D_a \quad [27]$$

where  $\tau$  is a tortuosity factor,  $\theta_a$  is air filled porosity, and  $D_a$  is water vapor diffusivity in air. The tortuosity factor can be described as (Millington and Quirk, 1961)

$$\tau = \frac{\theta_a^{7/3}}{\theta_s^2} \quad [28]$$

Since  $\theta_a$  and  $\theta_s$  are simple functions of  $\rho_b$  and soil water content, there is no influence of different soil type on  $D_v$ . Values for  $D_v$  decrease with increasing  $\rho_b$  because of the associated decrease in  $\theta_a$  (Fig. 10). When  $\theta$  is  $0.25 \text{ m}^3 \text{ m}^{-3}$ , a  $100 \text{ kg m}^{-3}$  increase of  $\rho_b$  caused 28.6%, 23.3%, and 24.9% decrease in  $D_v$  for clay loam, silt loam, and sandy loam, respectively. The  $D_v$  values for observed maximum  $\rho_b$  were 58.8%, 47.2%, and 53.6% of the values for observed minimum  $\rho_b$  for clay loam, silt loam, and sandy loam, respectively.

### Key Findings from Property Modeling

Six soil thermal and hydraulic properties were evaluated for three soil textures over a realistic range in transient field soil bulk density, using a combination of ten models/modeling approaches available from the literature. The properties that appeared to be most sensitive to bulk density are as follows:

- Thermal conductivity – change of <10% in bulk density led to 11-16% change in thermal

conductivity.

- Water characteristics – 25% change in bulk density led to 20-25% change in residual and saturated water contents, with changes occurring in opposite directions (i.e., larger residual water content and smaller saturated water content).
- Saturated hydraulic conductivity – values for saturated hydraulic conductivity typically change by an order of magnitude over the range of transient field bulk density.
- Vapor diffusivity – change of <10% in bulk density led to 23-29% change in diffusivity.

## NUMERICAL SIMULATIONS (Objective 2)

Simulations were performed with the HYDRUS-1D software package (Šimůnek et al., 2009) to evaluate impacts of change in bulk density on surface energy balance and soil heat and water transfer. Four soil profiles (A, B, C, and D) were used in the simulations, each approximately representing a soil with silt loam texture. The soil profiles have two layers (Fig. 11), one represents a disturbed soil layer (0-0.225 m depth) which has  $\rho_b = 1.3$  (A), 1.2 (B), 1.4 (C) or 1.5 (D)  $\text{Mg m}^{-3}$  bulk density, and the other is an undisturbed deep soil layer (0.225-5 m depth) which has  $\rho_b = 1.4 \text{ Mg m}^{-3}$ . (Thus, profile (C) has uniform  $\rho_b$  throughout the profile.) Node spacing was 0.01 m from surface through 50 cm depth, and node spacing was gradually increased to a maximum of 0.05 m below 50 cm depth. Hydraulic properties were expressed with the Brooks and Corey (1964) model, and parameters were obtained with the Assouline (2006a) approach described above. Thermal properties were calculated with the Campbell (1985) model.

Weather data from an experimental field near Ames, IA in 2012, 2013, and 2014 were used to determine surface boundary conditions. Calculations were made with data during May-October in each year. These three years provide differing amounts of precipitation during May-October. Accumulated precipitation in May-October was 337, 524, and 801 mm in 2012, 2013, and 2014, respectively, i.e., 2012 was a dry year, 2013 was intermediate, and 2014 was wet. Accumulated solar radiation during May-October was 3781, 3422, and 3216  $\text{MJ m}^{-2}$  in 2012, 2013, and 2014, respectively. The dry year (2012) had greater accumulated solar energy.

The soil surface boundary condition was determined by the calculated surface energy balance and the observed precipitation. The calculation processes are described in Šimůnek et al. (2009). The bottom boundary conditions were free drainage for water transport and zero gradient for heat transport. The initial condition for water content was  $0.25 \text{ m}^3 \text{ m}^{-3}$  for all depths and the initial condition for temperature was 20°C at all depths.

### Surface Energy Balance

Across all three years, *Net radiation* was smaller during the daytime and larger at night when  $\rho_b$  was low (not shown). The relatively small differences were likely associated with differences in surface albedo and longwave radiation from soil surface. *Ground heat flux* showed relatively large differences with  $\rho_b$  variation, particularly for dynamic fluxes within a given day (Fig. 12). Accumulated differences on an annual basis were relatively small (Table 4). In 2013 and 2014, ground heat flux was relatively small at  $\rho_b = 1.2 \text{ Mg m}^{-3}$ , and generally increased with  $\rho_b$  (Table 4). This may be associated with greater thermal conductivity with larger  $\rho_b$ . However, trends differed in 2012 when conditions were driest. In most cases smaller  $\rho_b$  produced larger *latent heat flux* (not shown). Accumulated latent heat flux (calculated as evaporation depth) was the highest with the lowest  $\rho_b$  in each simulated year (Table 4). This trend likely corresponds with increased storage of water available for evaporation from changes to the water characteristics

and with greater vapor diffusivity at low  $\rho_b$ . Based on these differences, surface energy partitioning shifted toward a relatively greater proportion of available energy partitioning to sensible heat flux when  $\rho_b$  was largest.

### **Soil Heat and Water Dynamics**

**Soil temperature** at the 5 cm soil depth generally showed greatest daily variation with low  $\rho_b$  (Fig. 13). Differences in temperature at maximum and minimum were typically on the order of 1 °C with low  $\rho_b$  having both the largest maximum and smallest minimum (i.e., difference in variation of 2 °C). At the 30 cm soil depth, where  $\rho_b$  was the same for each simulated profile, surface  $\rho_b$  also influenced observed temperatures (Fig. 14). However, in this case the trend was opposite that observed at the surface. At the 30 cm depth, daily temperature variation increased with high surface  $\rho_b$ . In this case, the surface layer with low  $\rho_b$ , and thus low thermal conductivity, acts as insulation, muting temperature variation in the subsurface. On a seasonal basis, high surface  $\rho_b$  results in earlier warming in the summer and earlier cooling in the fall (Fig. 15).

**Soil water content** at the 5 cm depth was generally drier at low  $\rho_b$  (Fig. 16). This result is likely a combination of both more rapid drainage during rainfall events, and lower residual water content retained. During a typical drying event, simulated water content at low  $\rho_b$  was about  $0.02 \text{ m}^3 \text{ m}^{-3}$  lower than at the largest  $\rho_b$  (Fig. 17). At the 30 cm depth, differences between profiles with different  $\rho_b$  were generally small (not shown).

### **Key Findings from Numerical Simulation**

Three seasons with differing surface conditions (rainfall, solar radiation) were simulated with a numerical model for a range of bulk density conditions. Main findings were that as bulk density increased:

- Ground heat flux increased by as much as 25% on an annual basis, though effects varied by year.
- Evaporation rate (latent heat flux) decreased by as much as 7-8% on an annual basis.
- Surface layer temperature variation decreased – differences in variation at the 5 cm depth were on the order of 2 °C.
- Subsurface layer temperature variation increased – even at 30 cm depth, the effect was on the order of 1 °C.
- Surface soil water content increased by about  $0.02 \text{ m}^3 \text{ m}^{-3}$  during typical drying events.

## BIBLIOGRAPHY

- Assouline, S. 2006a. Modeling the relationship between soil bulk density and the water retention curve. *Vadose Zone J.* 5:554-563.
- Assouline, S. 2006b. Modeling the relationship between soil bulk density and the hydraulic conductivity function. *Vadose Zone J.* 5:697-705.
- Berndt, R.D., and K.J. Coughlam. 1976. The nature of changes in bulk density with water content in a cracking clay. *Aust. J. Soil Res.* 15:27-37.
- Brooks, R. H., and A. T. Corey. 1964. Hydraulic properties of porous media. Hydrology Paper No. 3. Fort Collins, Colo.: Colorado State University.
- Campbell, G.S. 1985. *Soil Physics with BASIC*. Elsevier, New York
- de Vries, D.A. 1963. Thermal properties of soils. In: W.R. van Wijk, editor, *Physics of plant environment*. 2nd ed. North Holland Publ., Amsterdam. p. 210-235.
- Han, W., Y. Gong, T. Ren, and R. Horton. 2014. Accounting for time-variable soil porosity improves the accuracy of the gradient method for estimating soil carbon dioxide production. *Soil Sci. Soc. Am. J.* 78:1426-1433.
- Kay, B.D., C.D. Grant, and P.H. Groenevelt. 1985. Significance of ground freezing on soil bulk density under zero tillage. *Soil Sci. Soc. Am. J.* 49:973-978.
- Liu, X., S. Lu, R. Horton, and T. Ren. 2014. In situ monitoring of soil bulk density with a thermo-TDR sensor. *Soil Sci. Soc. Am. J.* 78:400-407.
- Logsdon, S.D. 2012. Temporal variability of bulk density and soil water at selected field sites. *Soil Sci.* 177:327-331.
- Lu, Y., S. Lu, R. Horton, and T. Ren. 2014. An empirical model for estimating soil thermal conductivity from texture, water content, and bulk density. *Soil Sci. Soc. Am. J.* 78:1859-1868.
- Ma, L., L.R. Ahuja, B.T. Nolan, R.W. Malone, T.J. Trout, and Z. Qi. 2012. Root zone water quality model (RZWQM2): model use, calibration, and validation. *Trans. ASABE* 55:1425-1446.
- Millington, R.J., and J.P. Quirk. 1961. Permeability of porous media. *Trans. Faraday Soc.* 57:1200-1207.
- Moldrup, P., T. Olesen, J. Gamst, P. Schjønning, T. Yamaguchi and D.E. Rolston. 2000. Predicting the gas diffusion coefficient in repacked soil water-induced linear reduction model. *Soil Sci. Soc. Am. J.* 64:1588-1594.
- Mualem, Y. 1976. A new model for predicting the hydraulic conductivity of unsaturated porous media. *Water Resour. Res.* 12:513-522.
- Schaap, M.G., F.J. Leij, and M. Th. van Genuchten. 2001. ROSETTA: a computer program for estimating soil hydraulic parameters with hierarchical pedotransfer functions. *J. Hydrol.* 251:163-176.
- Šimůnek, J., M. Šejna, H. Saito, M. Sakai, and M. Th. van Genuchten. 2009. The HYDRUS-1D software package for simulating the one-dimensional movement of water, heat, and multiple solutes in variably saturated media. Version 4.08. [http://www.pc-progress.com/Downloads/Pgm\\_hydrus1D/HYDRUS1D-4.08.pdf](http://www.pc-progress.com/Downloads/Pgm_hydrus1D/HYDRUS1D-4.08.pdf)
- van Genuchten, M.Th. 1980. A closed-form equation for predicting the hydraulic conductivity of unsaturated soils. *Soil Sci. Soc. Am. J.* 44:892-898.
- Wösten, J.H.M., A. Lilly, A. Nemes, and C. Le Bas. 1999. Development and use of a database of hydraulic properties of European soils. *Geoderma* 90:169-185.

**Table 1. Soil particle size distribution, soil organic matter content (SOM), and observed minimum and maximum values for soil bulk density.**

Texture	Particle size distribution			SOM kg kg <sup>-1</sup>	Bulk density kg m <sup>-3</sup>	
	Sand	Silt	Clay		Min	Max
Clay loam	21	47	32	0.07	1250	1400
Silt loam	17	62	21	0.01	1100	1350
Sandy loam	53	38	9	0.01	1150	1350

**Table 2. Empirical parameters for the van Genuchten (1980) model output with ROSETTA (Schaap et al., 2001) as a function of soil bulk density.**

Parameter	Bulk density Mg m <sup>-3</sup>		
	1.1	1.25	1.4
	<i>Clay loam</i>		
$\theta_r$	0.091	0.088	0.084
$\theta_s$	0.522	0.480	0.441
$K_s$ (cm d <sup>-1</sup> )	53.2	22.5	9.6
	<i>Silt loam</i>		
$\theta_r$	0.078	0.074	0.071
$\theta_s$	0.495	0.455	0.419
$K_s$ (cm d <sup>-1</sup> )	70.5	33.7	15.8
	<i>Sandy loam</i>		
$\theta_r$	0.045	0.042	0.040
$\theta_s$	0.442	0.432	0.377
$K_s$ (cm d <sup>-1</sup> )	121	68.8	40.1

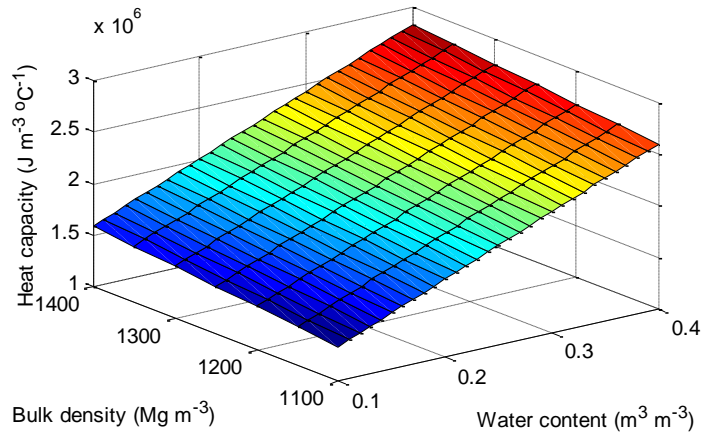
**Table 3. Empirical parameters for the Assouline (2006) approach as a function of soil bulk density. Parameters at bulk density = 1.25 Mg m<sup>-3</sup> were estimated with ROSETTA (Schaap et al., 2001).**

Parameter	Bulk density		
	1.1	1.25	1.4
	Mg m <sup>-3</sup>		
	<i>Clay loam</i>		
$\theta_r$	0.080	0.088	0.102
$\theta_s$	0.531	0.480	0.428
$\psi_a$ (cm)	52.2	85.0	131
$\sigma$	0.47	0.52	0.57
$K_s$ (cm d <sup>-1</sup> )	76.1	22.5	6.82
	<i>Silt loam</i>		
$\theta_r$	0.067	0.074	0.085
$\theta_s$	0.504	0.455	0.406
$\psi_a$ (cm)	90.3	147	227
$\sigma$	0.546	0.63	0.72
$K_s$ (cm d <sup>-1</sup> )	106	33.7	10.8
	<i>Sandy loam</i>		
$\theta_r$	0.040	0.042	0.051
$\theta_s$	0.452	0.408	0.365
$\psi_a$ (cm)	40.4	65.8	102
$\sigma$	0.42	0.51	0.59
$K_s$ (cm d <sup>-1</sup> )	193	68.8	24.6

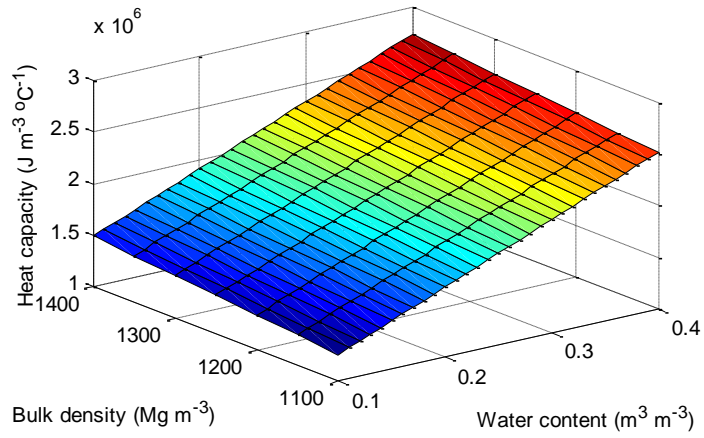
**Table 4. Accumulated ground heat flux (positive downward) and evaporation as a function of soil bulk density for May to October in each simulation year.**

Year	Soil bulk density (surface)			
	Mg m <sup>-3</sup>			
	1.1	1.3	1.4	1.5
	Cumulative ground heat flux			
	MJ m <sup>-2</sup>			
2012	13.4	13.3	13.1	13.2
2013	6.0	5.7	6.1	6.4
2014	-4.6	-4.1	-3.7	-3.6
	Cumulative evaporation			
	mm			
2012	390	380	371	363
2013	576	569	563	557
2014	858	854	852	849

(a) Clay loam



(b) Silt loam



(c) Sandy loam

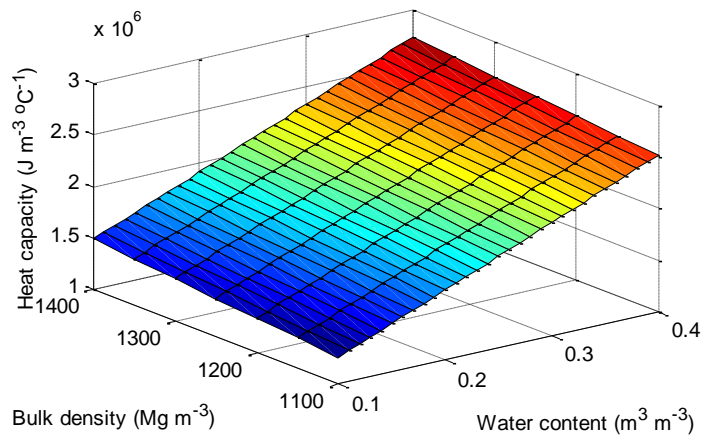
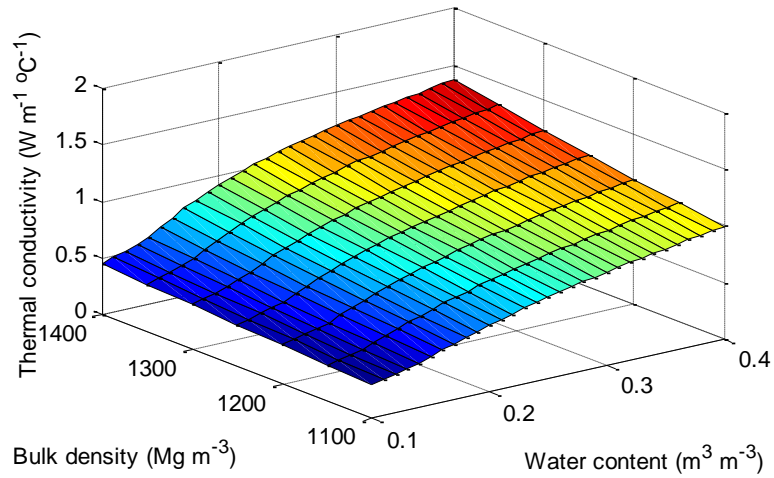
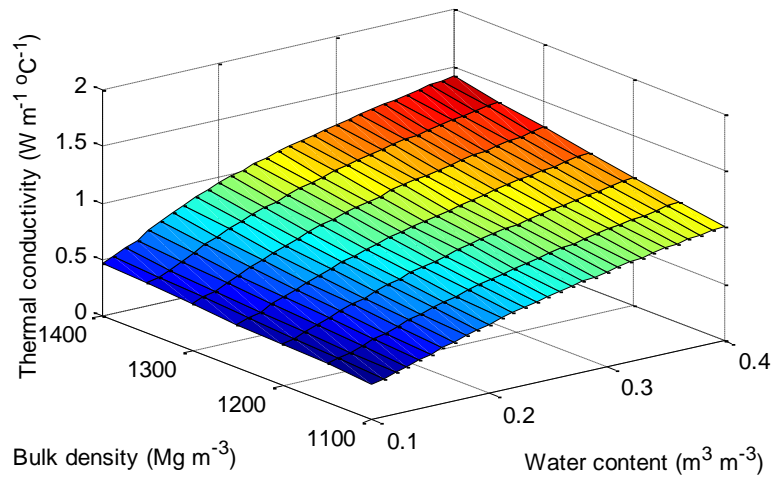


**Figure 1. Volumetric heat capacity as a function of bulk density and volumetric water content.**

(a) Clay loam



(b) Silt loam



(c) Sandy loam

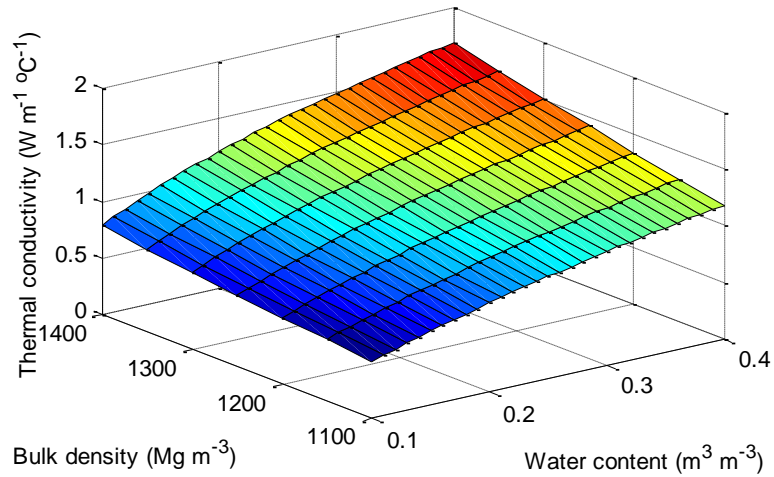
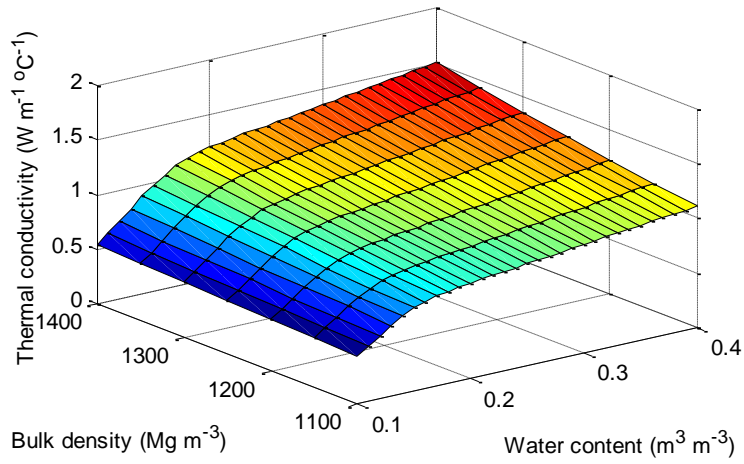
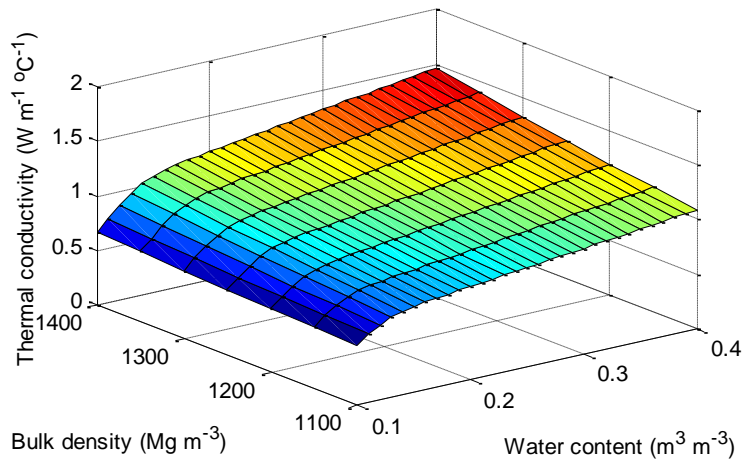


**Figure 2. Thermal conductivity as a function of bulk density and volumetric water content with de Vries (1963) model.**

(a) Clay loam



(b) Silt loam



(c) Sandy loam

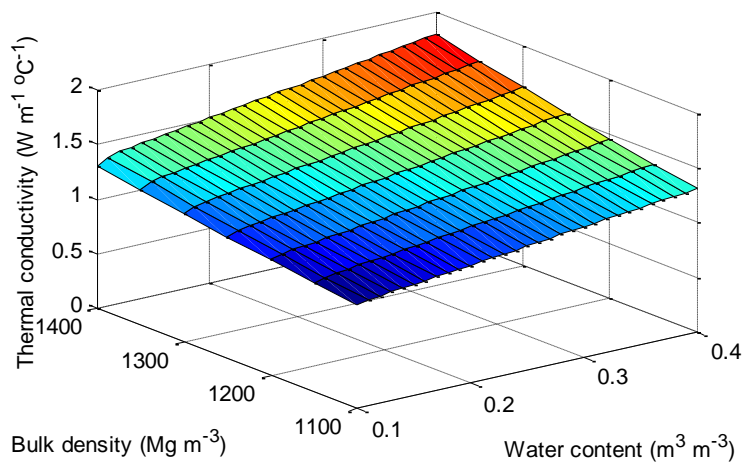


**Figure 3. Thermal conductivity as a function of bulk density and volumetric water content with Campbell (1985) model.**

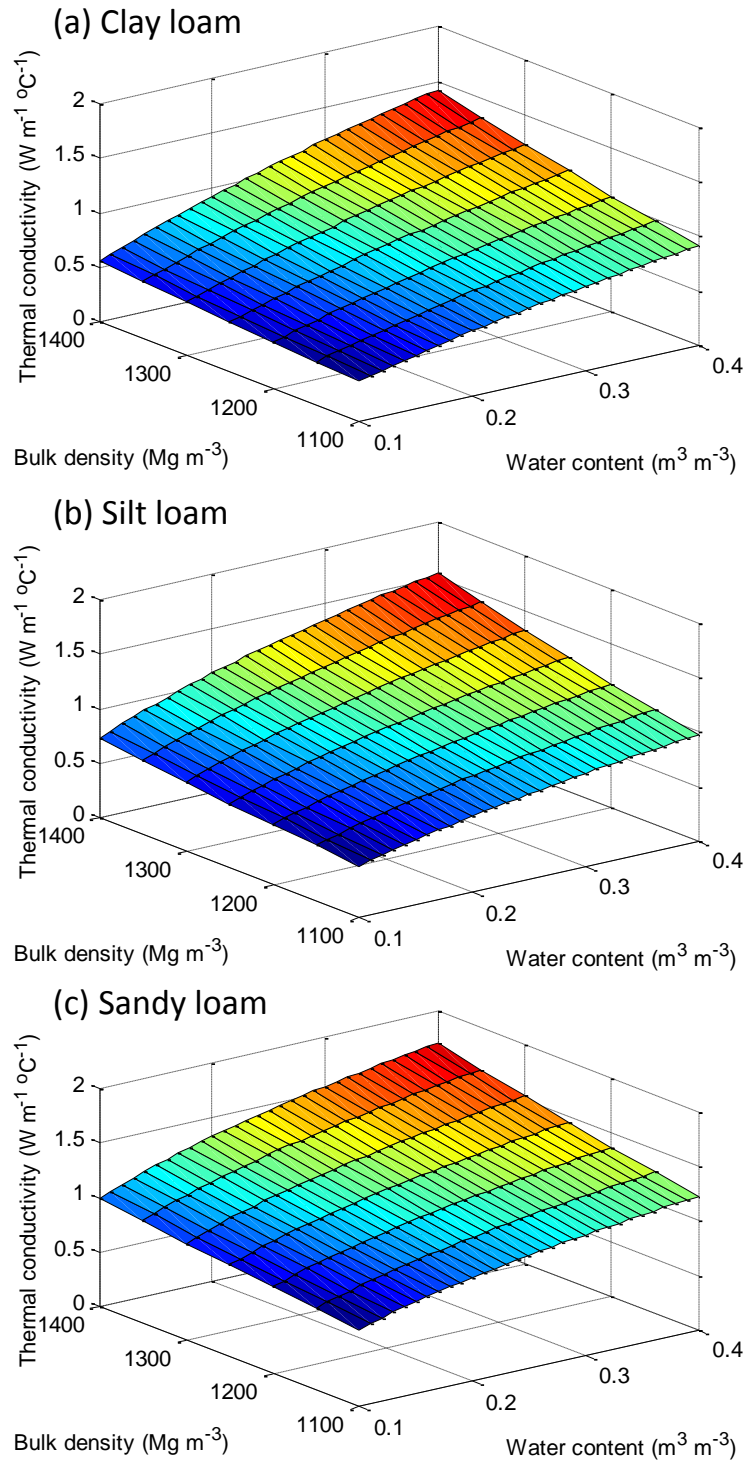
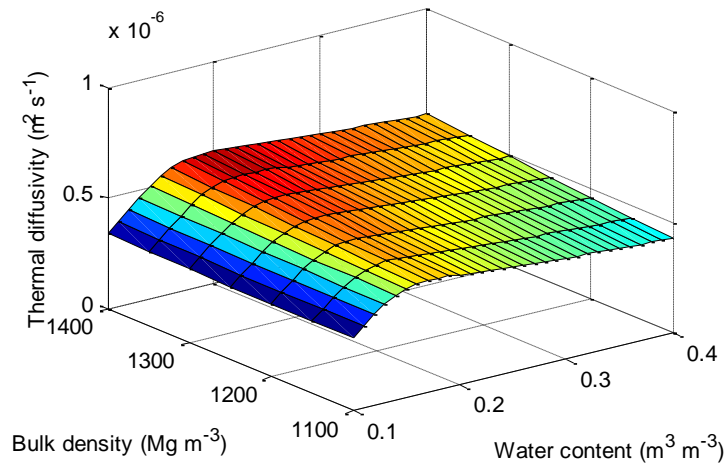
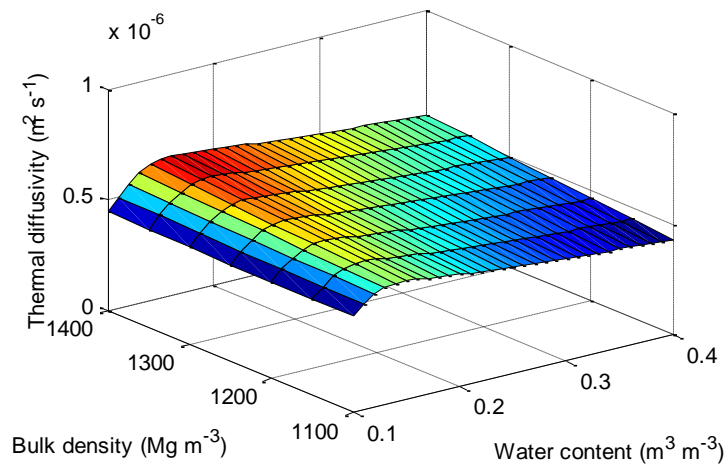


**Figure 4. Thermal conductivity as a function of bulk density and volumetric water content with Lu et al. (2014) model.**

(a) Clay loam



(b) Silt loam



(c) Sandy loam

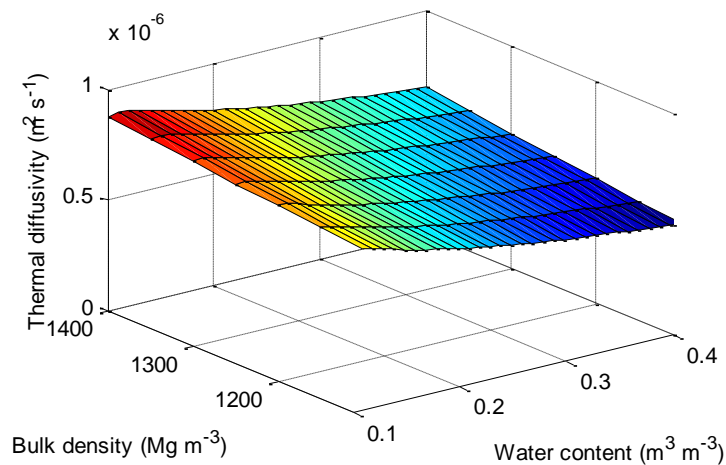


**Figure 5. Thermal diffusivity as a function of bulk density and volumetric water content based on thermal conductivity determined with Campbell (1985) model and heat capacity determined with the de Vries (1963) model.**

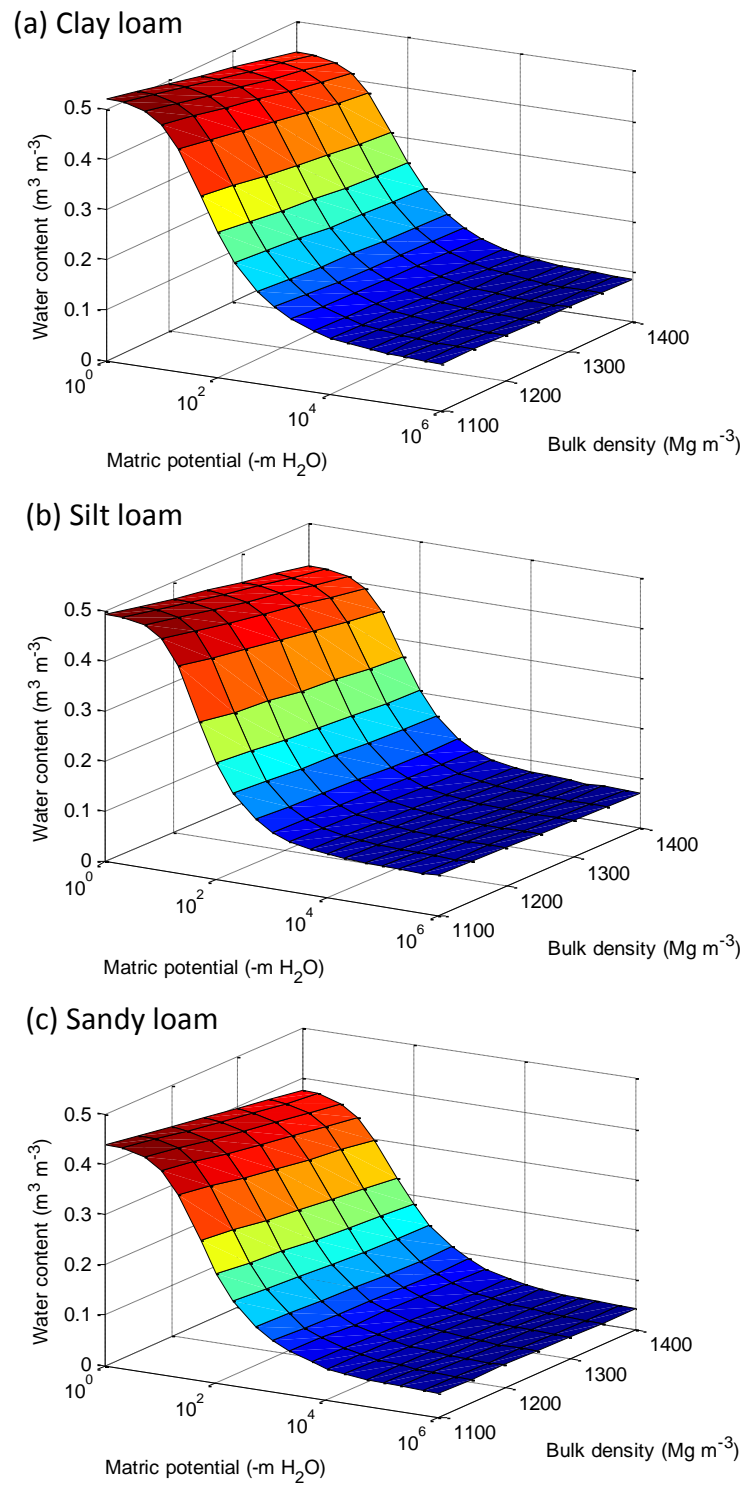


**Figure 6. Water characteristics estimated with ROSETTA (Schaap et al., 2001) for different values of soil bulk density.**

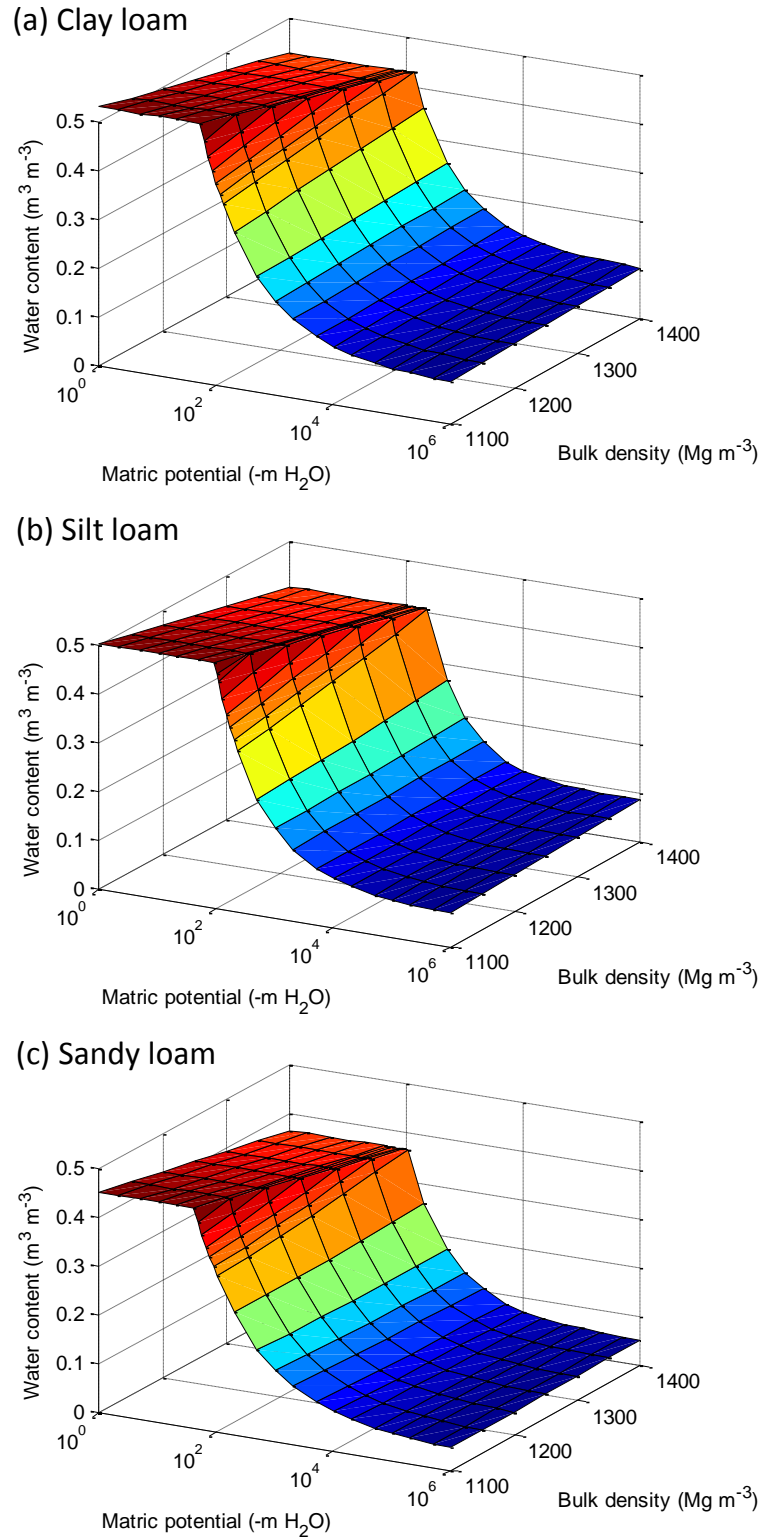


**Figure 7. Water characteristics estimated with Assouline (2006a) and Brooks and Corey (1964) models at different values for bulk density.**

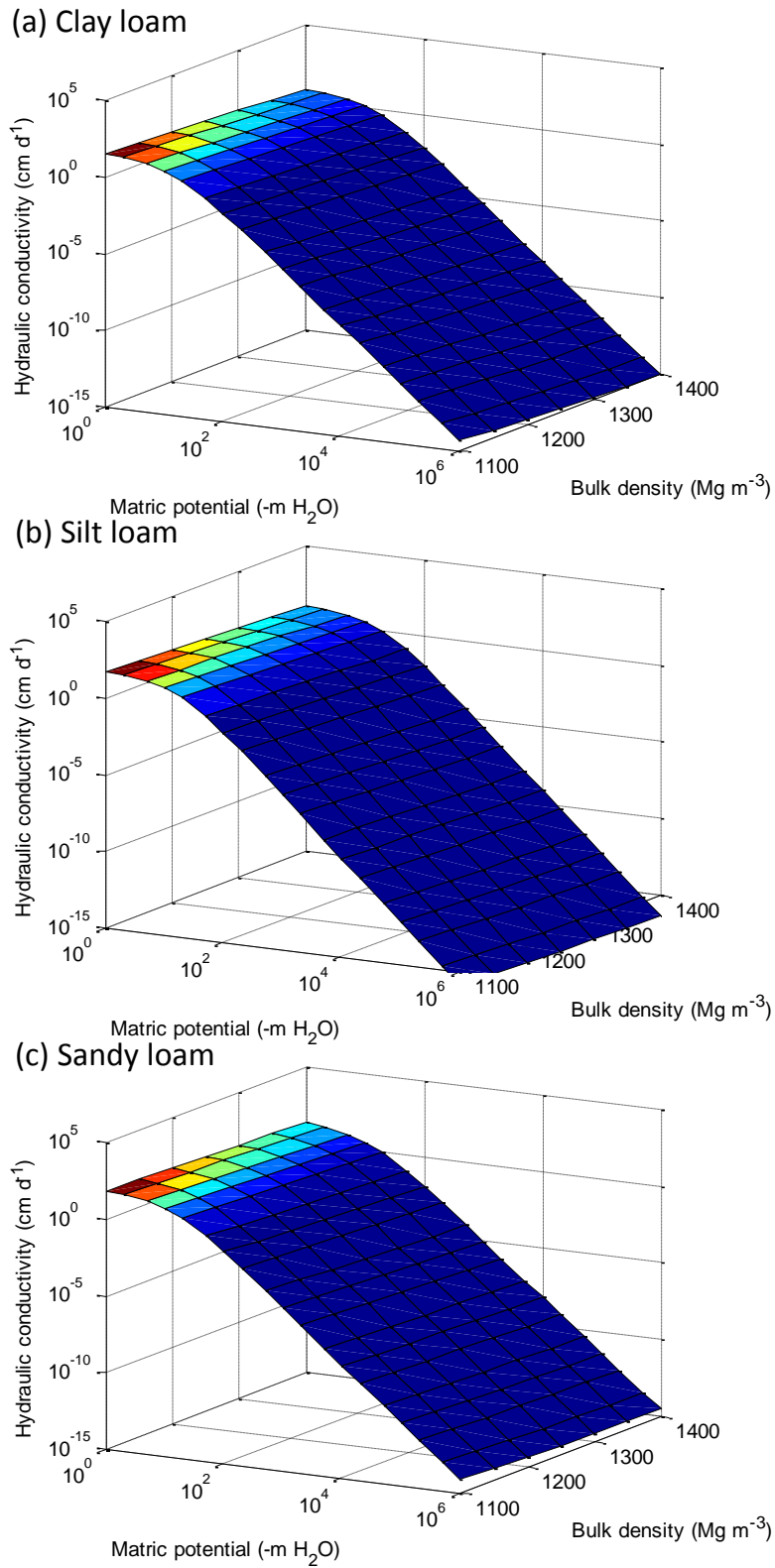
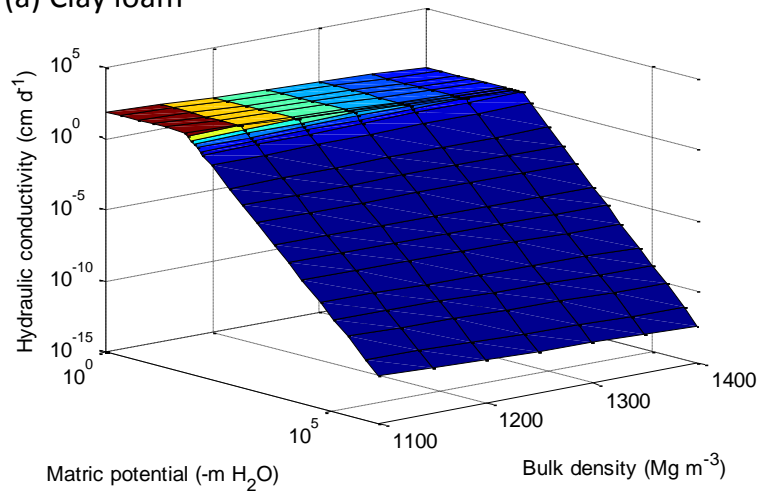
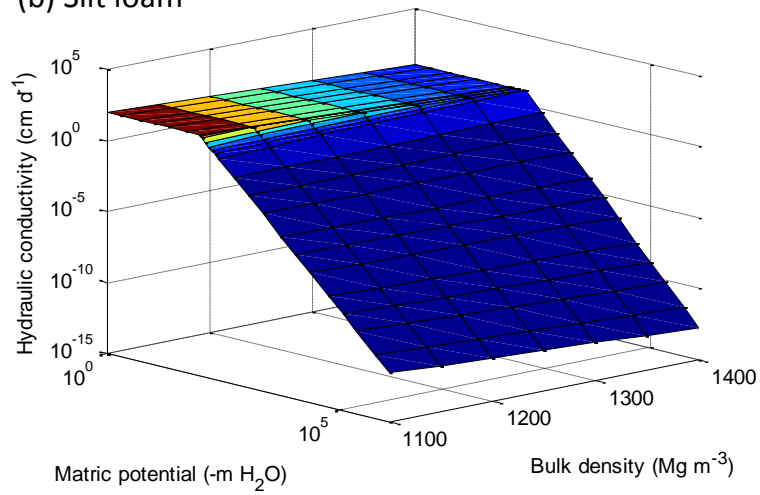


**Figure 8. Hydraulic conductivity estimated with ROSETTA for different values of bulk density.**

(a) Clay loam



(b) Silt loam



(c) Sandy loam

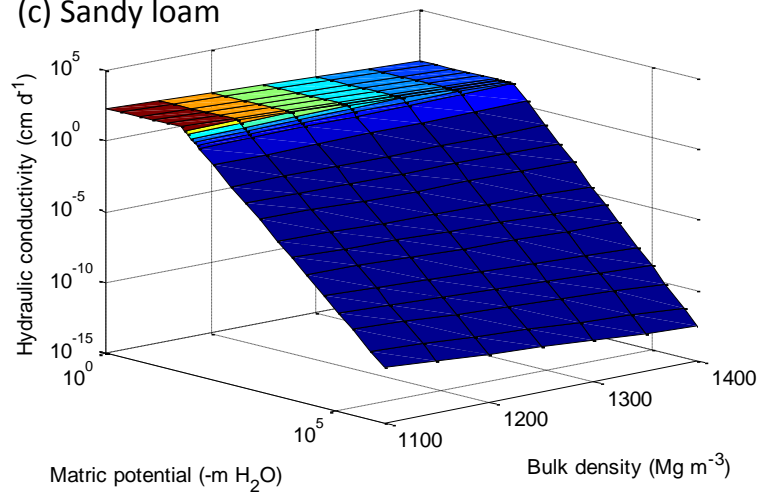


**Figure 9. Hydraulic conductivity with Mualem (1976) and Brooks and Corey (1964) models with different values for bulk density.**

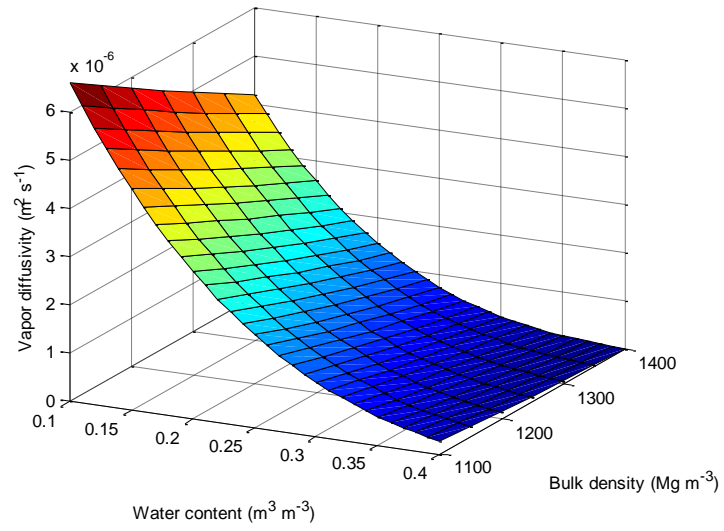


**Figure 10. Vapor diffusivity in soil with different values for bulk density.**

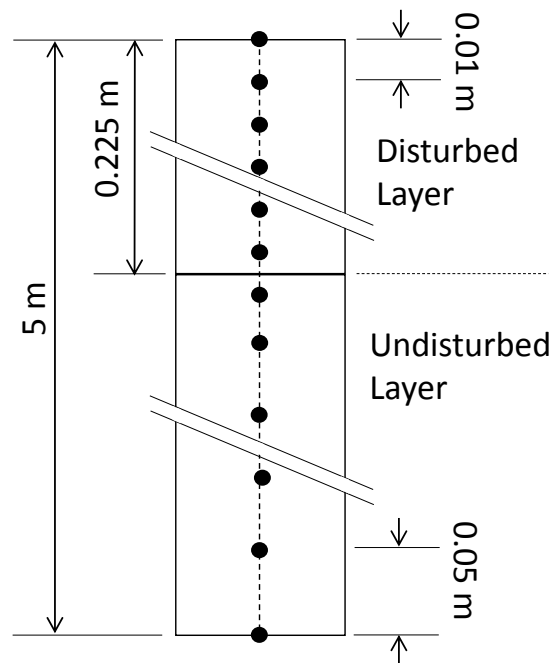


**Figure 11. Soil profile used in the HYDRUS-1D simulations. A has a uniform soil properties, and B and C have disturbed layer and undisturbed layer.**

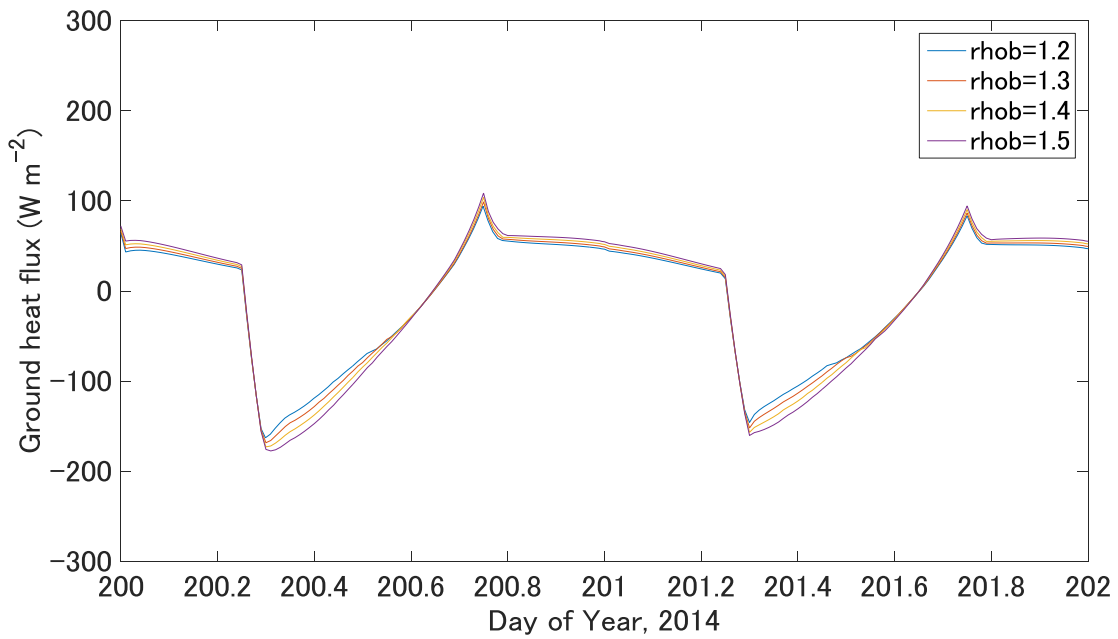
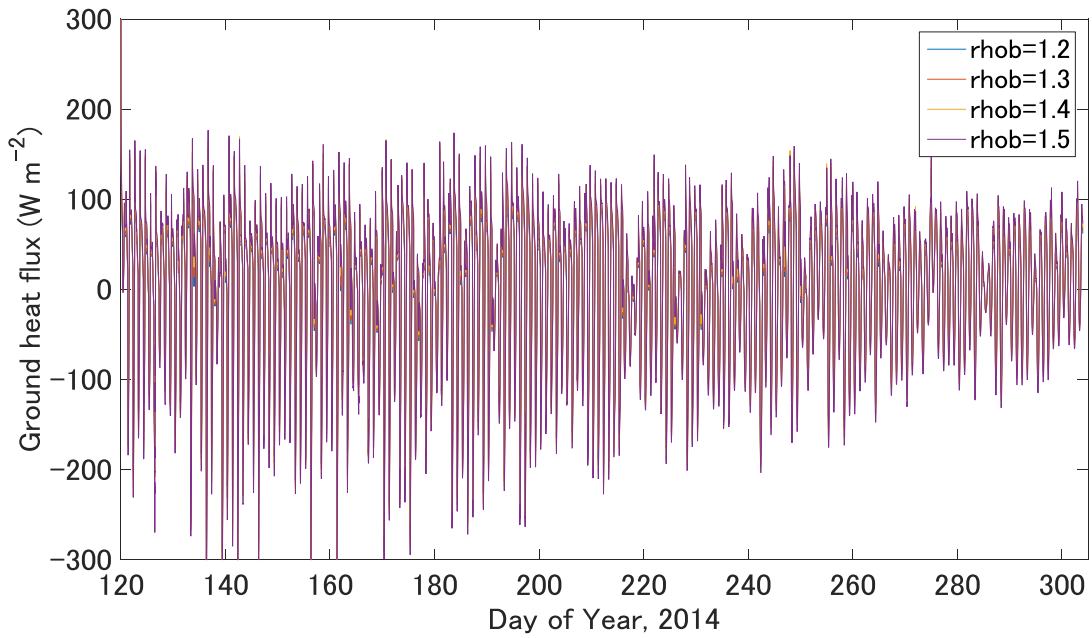


**Figure 12. Simulated ground heat flux; positive values indicated downward heat flux. Top: May through October, bottom: day of year 200 to 202. Legends indicate bulk density (rhob) in Mg m<sup>-3</sup>.**

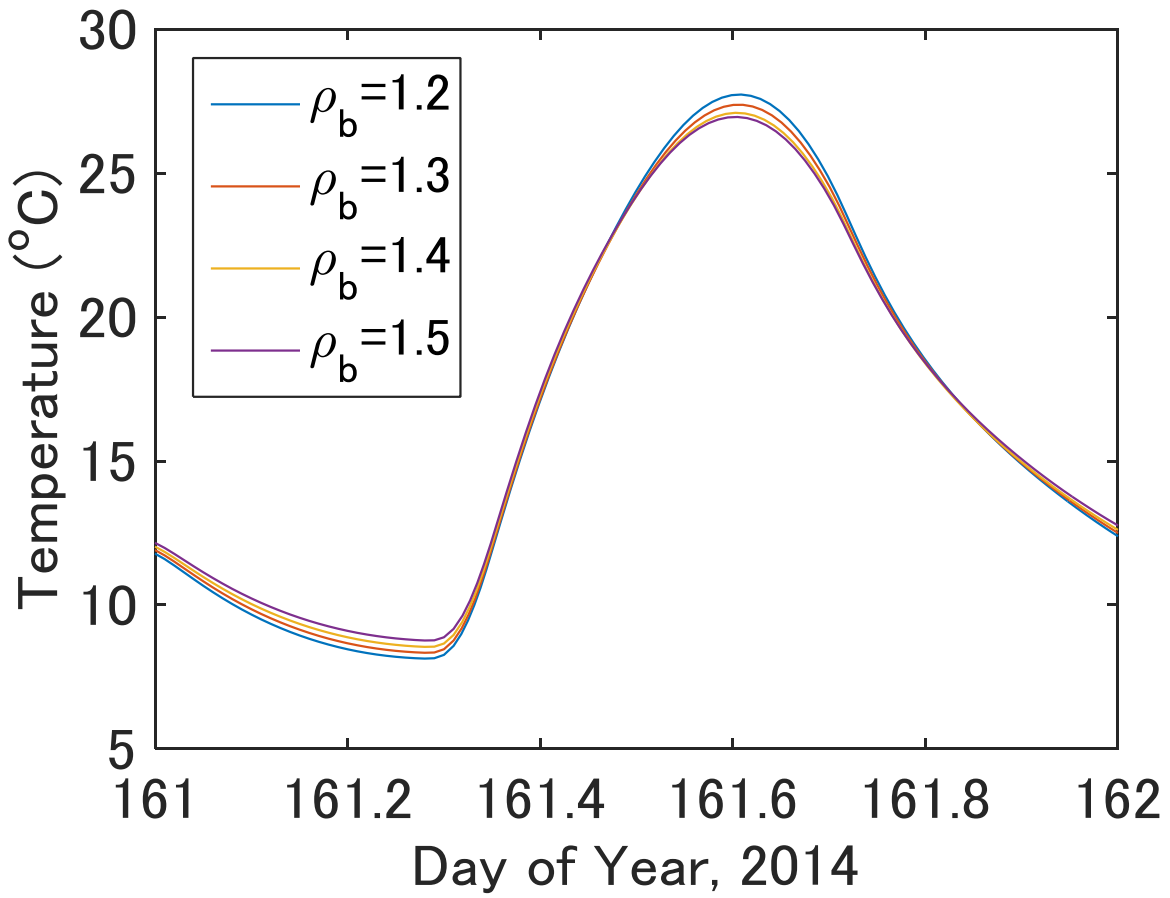


Figure 13. Simulated daily soil temperature at 5 cm soil depth. Legend indicates bulk density ( $\rho_b$ ) in  $\text{Mg m}^{-3}$ .

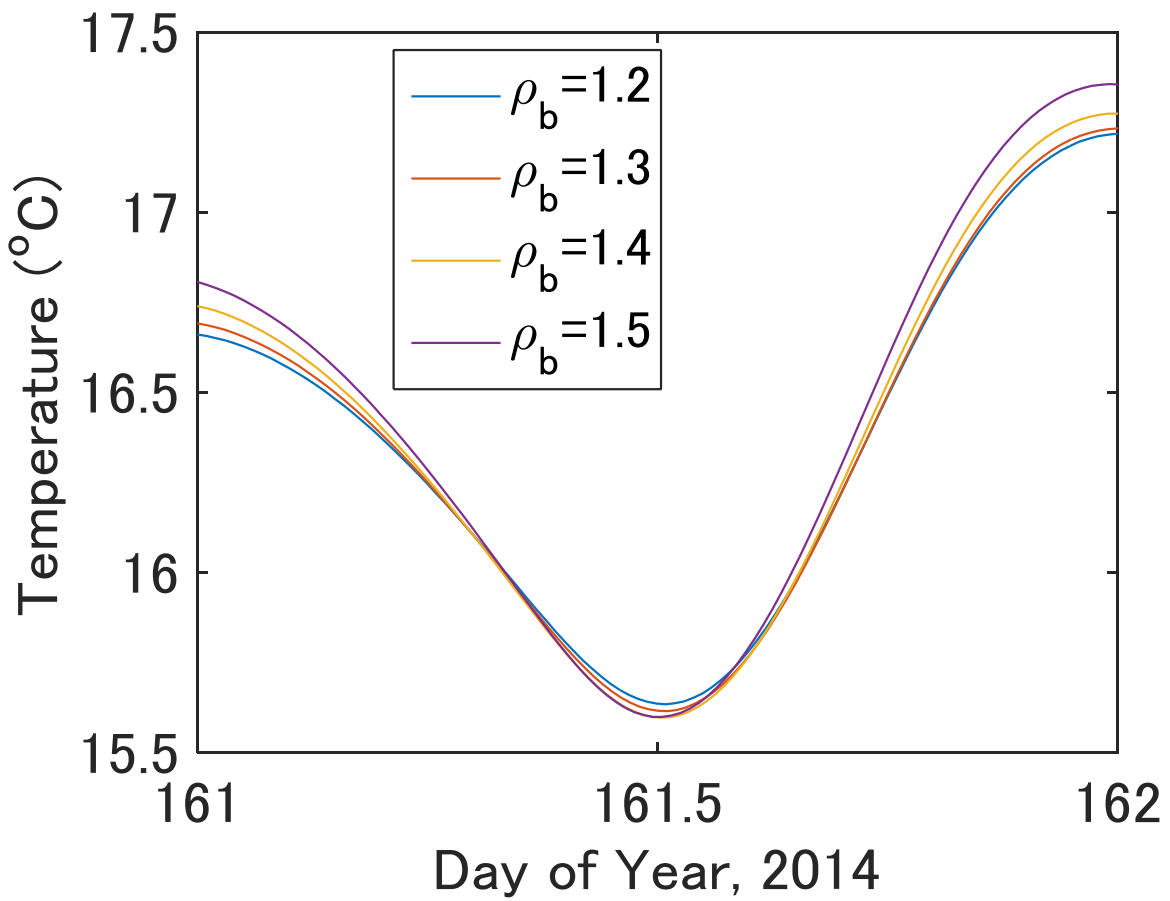


Figure 14. Simulated daily soil temperature at 30 cm soil depth. Legend indicates bulk density ( $\rho_b$ ) in  $\text{Mg m}^{-3}$ .

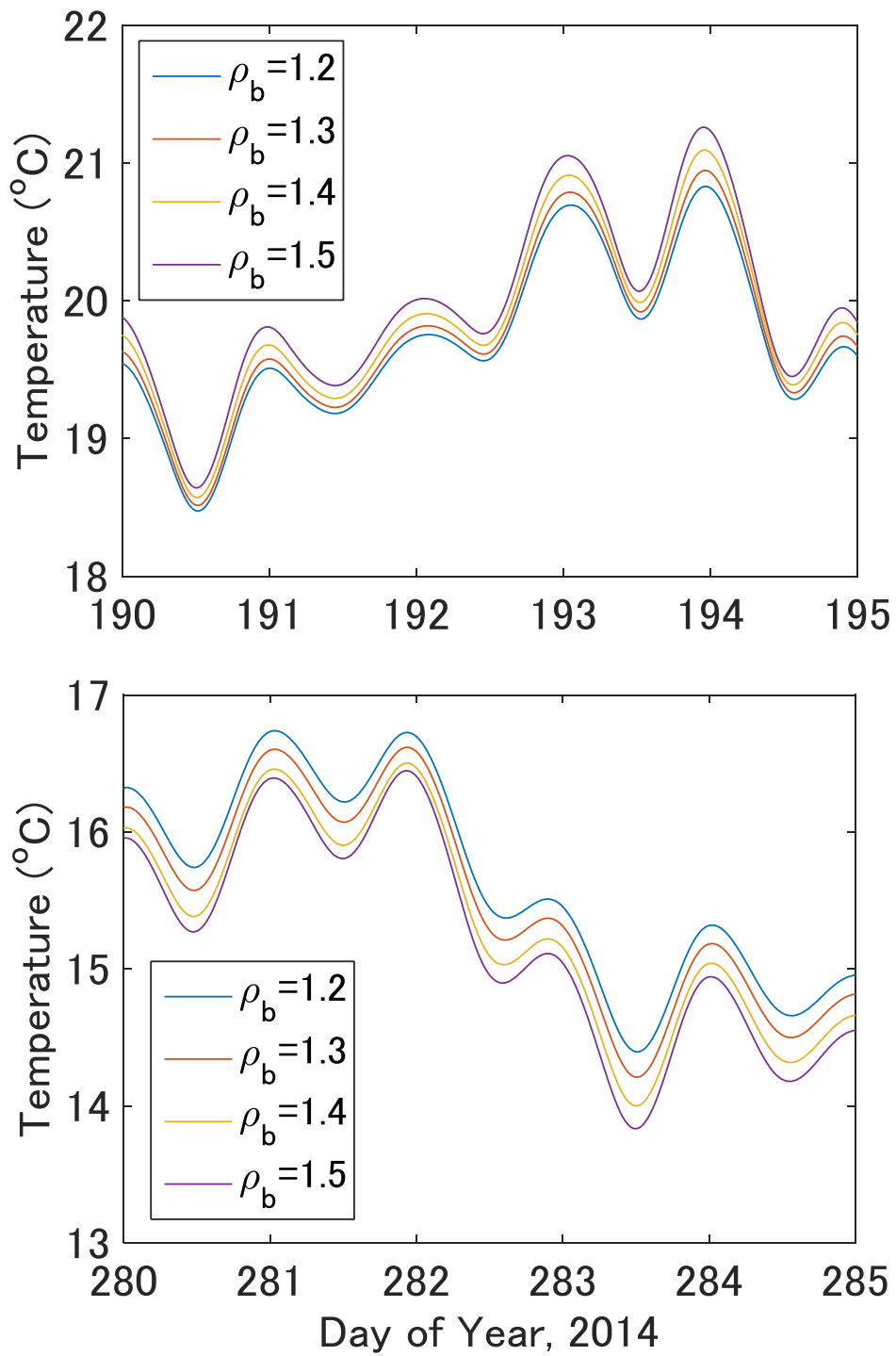
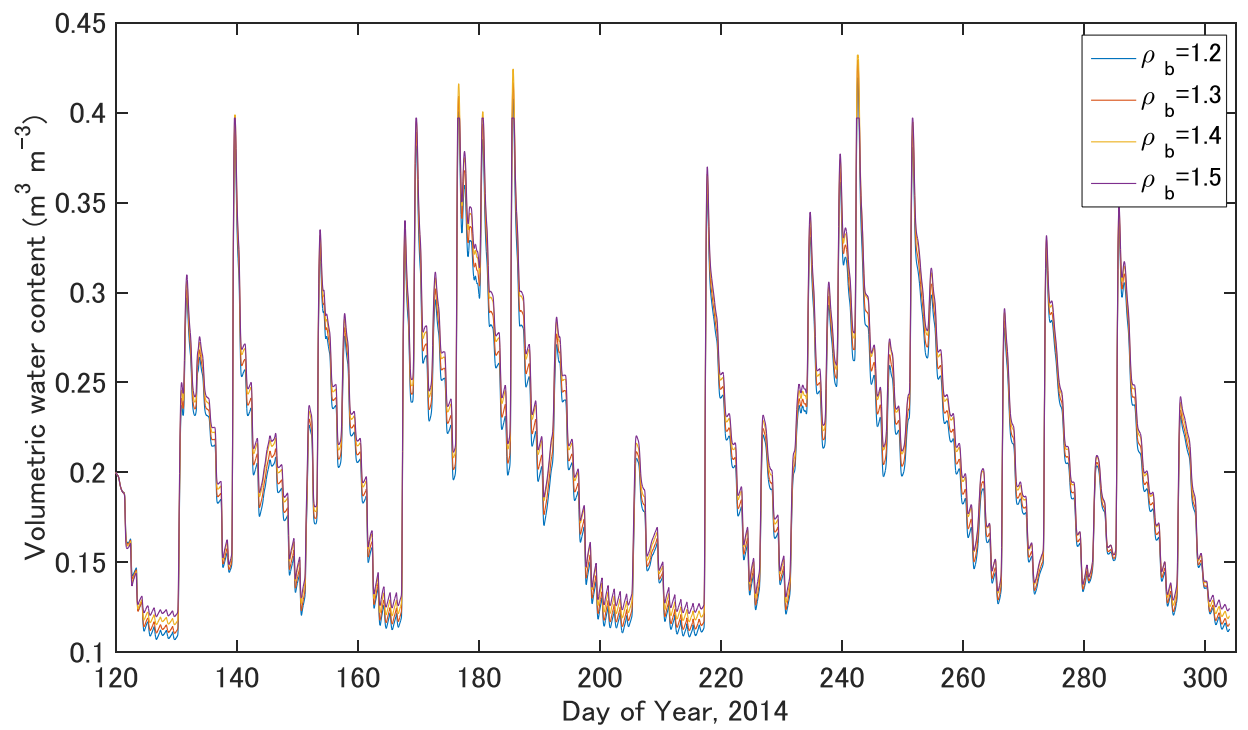
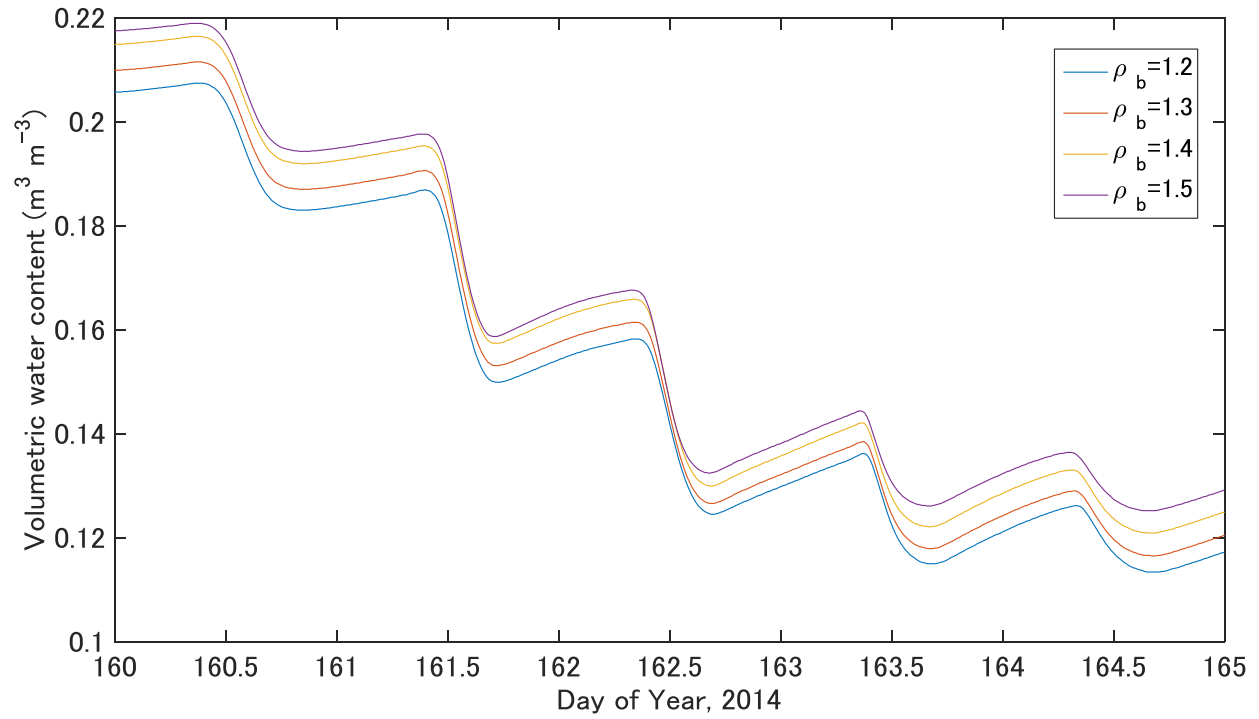


Figure 15. Simulated seasonal soil temperature at 30 cm soil depth. Top: summer, bottom: fall. Legend indicates bulk density ( $\rho_b$ ) in  $\text{Mg m}^{-3}$ .



**Figure 16. Simulated seasonal soil water content at 5 cm soil depth. Legend indicates bulk density ( $\rho_b$ ) in  $\text{Mg m}^{-3}$ .**



**Figure 17. Simulated soil water content at 5 cm soil depth during a drying event. Legend indicates bulk density ( $\rho_b$ ) in  $\text{Mg m}^{-3}$ .**